ELSEVIER

Journal of Nuclear Materials 258–263 (1998) 1163–1166

journal of nuclear materials

Irradiation creep of various ferritic alloys irradiated at ~400°C in the PFR and FFTF reactors

M.B. Toloczko [a,b,*], F.A. Garner [b], C.R. Eiholzer [b]

[a] *Washington State University, Pullman, WA 99163, USA*

[b] *Pacific Northwest National Laboratory, Battelle PNNL, MS p8-15, P.O. Box 999, Richland, WA 99352, USA*

Abstract

Irradiation creep of three ferritic alloys at ~400°C has been studied. Specimens were in the form of pressurized tubes. In a joint US/UK creep study, two identical sets of creep specimens constructed from one heat of HT9 were irradiated in fast reactors, one in the Prototypic Fast Reactor (PFR) and the other in the Fast Flux Test Facility (FFTF). The specimens in PFR were irradiated to a dose of ~50 dpa, whereas the specimens in FFTF were irradiated to a dose of 165 dpa. The observed swelling and creep behavior were very different in the two reactors. Creep specimens constructed from D57, a developmental alloy ferritic alloy, were also irradiated in PFR to a dose of ~50 dpa. Creep behavior typical of previous studies on ferritic alloys was observed. Finally, creep specimens constructed from MA957, a Y_2O_3 dispersion-hardened ferritic alloy, were irradiated in FFTF to a dose of ~110 dpa. This alloy exhibited a large amount of densification, and the creep behavior was different than observed in more conventional ferritic or ferritic–martensitic alloys.

1. Introduction

Ferritic alloys are under consideration for use in the first wall of fusion devices [1,2]. Compared to austenitic alloys which are also under consideration for first wall structures [3], relatively less irradiation creep data on ferritic alloys has been published. The purpose of this work is to add to the published data base on the general behavior of irradiation creep in ferritic alloys.

2. Experimental details

Summarized in Table 1 are the compositions and heat treatments of the three ferritic alloys. HT9 is a commercial ferritic–martensitic alloy, whereas D57 is a developmental ferritic alloy containing large amounts of molybdenum and is strengthened by the formation of secondary Laves phase (Fe_2Mo). MA957 is an experimental Y_2O_3 (yttria) dispersion-hardened ferritic alloy. MA957 is also unique in that during the construction of the pressurized tubes, a highly elongated grain structure is formed [4]. Tubing with 4.57 mm OD × 4.17 mm ID was used to construct the HT9 and D57 specimens, while tubing with 5.84 mm OD × 5.08 mm ID was used to construct the MA957 specimens. The tubes were capped, welded, and pressurized to operate at hoop stresses ranging from 0–200 MPa at the target irradiation temperature. A tube-set typically contains four to eight pressurized tubes with one tube pressurized to operate at the irradiation temperature with a hoop stress of 0 MPa. In general, a tube-set is kept together during the entire irradiation sequence.

In PFR, the Demountable Subassembly (DMSA) irradiation vehicle was utilized and is described in detail in Ref. [5]. This vehicle is essentially a heat pipe, and specimens are located at various axial positions in and near the reactor core. Tube-sets placed near the core center experienced higher fluxes. Temperature control in this vehicle was passive. Thermocouples were placed at the coolant inlet and outlet to the vehicle, and the reported temperature was the dose-weighted average of these inlet and outlet temperatures. The coolant inlet and outlet temperatures were not available to the authors for analysis, and without these details, it was not possible to more accurately estimate the specimen

* Corresponding author. Tel.: +1 509 376 0156; fax: +1 509 376 0418; e-mail: mic@wsunix.wsu.edu.

0022-3115/98/$19.00
PII: S0022-3115(98)00165-2

Table 1
Compositions and heat treatments of alloys

Alloy	Heat	Ni	Cr	Mn	Mo	Si	C	V	W	Nb	Ti	Y_2O_3
HT9 [a]	91353	0.51	11.8	0.50	1.03	0.21	0.21	0.33	0.52	–		–
D57 [b]	K168	0.64	9.7	0.27	5.57	0.32	0.07	0.56	–	0.54		–
MA957 [c]	DBB0111	0.13	13.87	0.05	0.30	0.05	0.014	–	–	–	1.05	0.22

[a] 1038°C/5 min/AC +760°C/30 min/AC.
[b] 1038°C/2 min/AC +25% CW.
[c] 760°C/360 min/AC.

temperatures. Thus, it is possible that in addition to flux variations, small temperature variations may have also existed between tube-sets placed at widely separated positions along the heat pipe.

For the PFR irradiations, two tube-sets were irradiated at different axial locations in the heat pipe. The original intent of this procedure was to supply two dose levels in one irradiation cycle. However, this procedure ignores the effect of flux on swelling, and this flux effect does not always allow data produced at different flux levels to be combined and analyzed as if it were flux-independent [6]. For purposes of this work, the tube-sets at the different axial locations are simply treated as different tube-sets. A schematic showing the basic placement of two tube-sets in the heat pipe is shown in Fig. 1. Volume constraints in the heat-pipe allowed only four tubes at a given reactor axial level, and tube-sets comprised of more than four tubes were divided between two adjacent axial locations, as depicted in Fig. 1. Although the subsets are adjacent, the difference in position resulted in small flux variations and probably very small temperature differences.

In FFTF, pressurized tubes were irradiated side-by-side. The irradiation temperature may vary slightly from one irradiation cycle to the next, but during any one cycle, the temperature was actively controlled to within ±5°C. The FFTF-MOTA is described in Ref. [7].

Swelling and creep strains were calculated from diameter measurements of the tubes after each irradiation cycle. These measurements were performed using a laser profilometry technique that is described elsewhere [7]. For the pressurized tubes used in this study, the uncertainty in the diameter measurement is less than ±0.5% of the measurement [8].

Swelling was estimated from diameter measurement of the stress-free tube in each tube-set. This is not an optimal method for swelling measurement because stress-enhanced swelling may have occurred in the stressed tubes. With the stress-free swelling estimate, irradiation creep can be estimated by removing the "swelling strain" from the total diametral strain measured in a pressurized tube.

3. Results

3.1. Stress-free tubes

Volume changes of the stress-free tubes, as estimated from diameter changes, and assuming isotropic strain

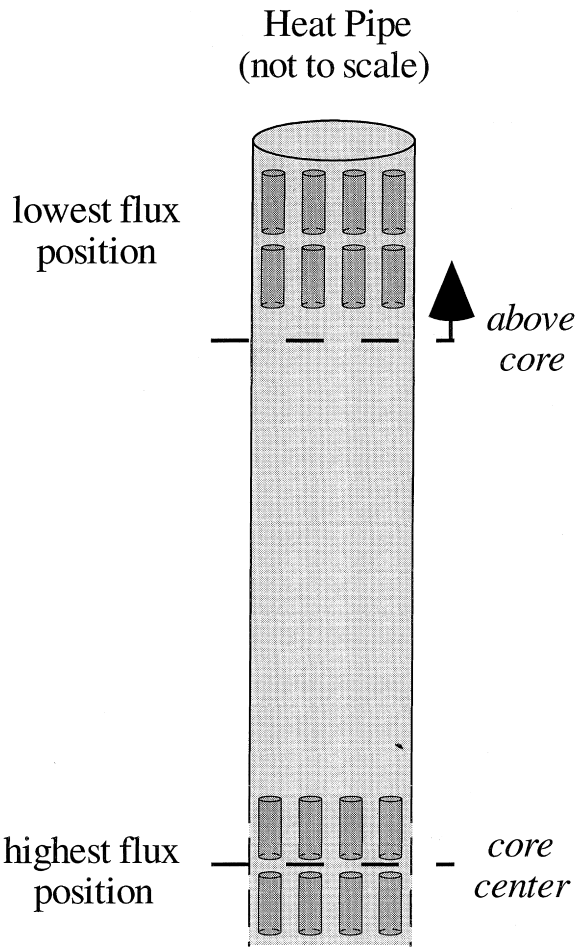

Fig. 1. Schematic of tube locations in the DMSA heat pipe.

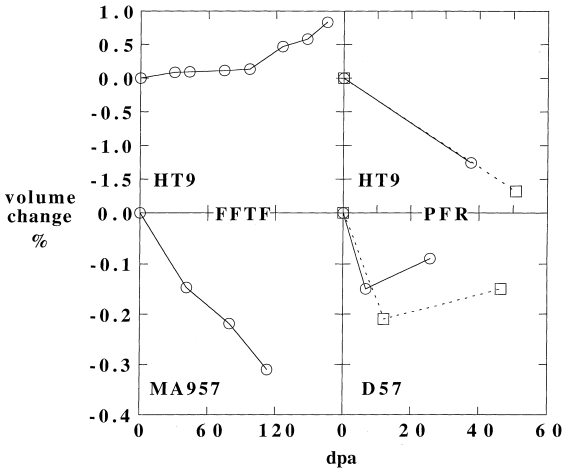

Fig. 2. Volume change of stress-free tubes, estimated from the diameter change assuming isotropic behavior. Note different scales on both axes.

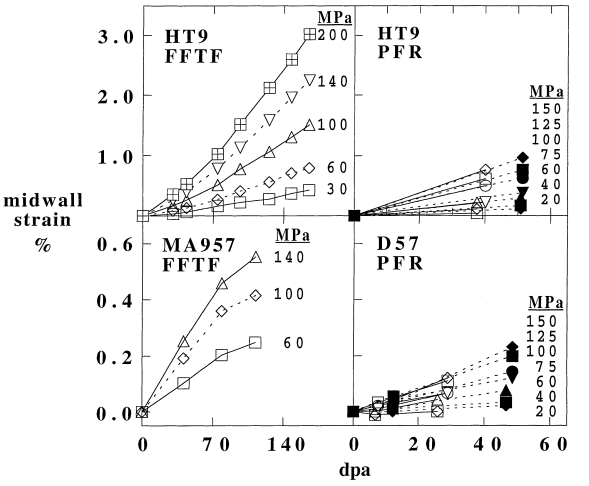

Fig. 3. Midwall creep strains versus dose. Note different scales on both axes.

behavior, are shown in Fig. 2. Three types of behavior were observed. The first, as demonstrated by the HT9 irradiated in FFTF, is a small positive transient followed by a long incubation period. The second, as shown by the D57 irradiated in PFR, is a small negative transient followed by a similar incubation period. Finally, the FFTF-irradiated MA957 displayed a continuous apparent densification behavior over the entire irradiation history. The PFR-irradiated HT9 probably exhibited densification similar to that observed in the D57.

The FFTF-irradiated HT9 stress-free tube is the only one that exhibited any apparent swelling. However, in the stress-free tubes of the other alloys, a small amount of swelling may have occurred and been overwhelmed by a larger amount of negative strain.

3.2. Irradiation creep behavior

The observed irradiation creep behavior is relatively typical of that previously observed in ferritic martensitic alloys [8,9]. Fig. 3 shows the midwall creep strains plotted versus dose, while Fig. 4 shows the midwall creep strains plotted versus hoop stress. Irradiation creep was linear with stress over the range of stresses examined. The MA957 alloy was unusual in that the creep rate appears to decrease with increasing dose.

4. Discussion

4.1. Stress-free tubes

Irradiation of the same heat of HT9 in both PFR and FFTF offers a unique study of irradiation history effects.

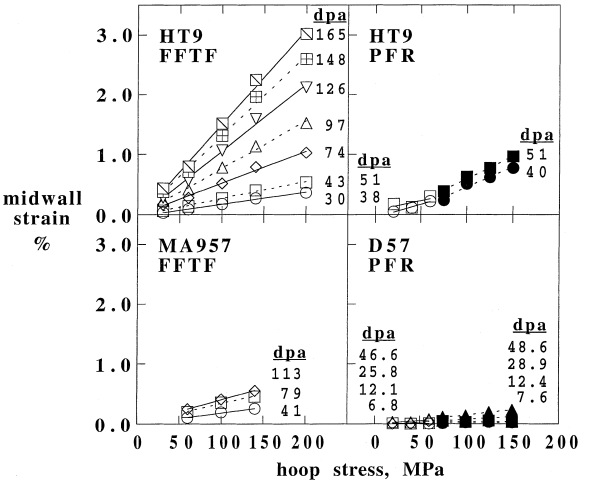

Fig. 4. Midwall creep strains versus hoop stress. Note slightly different scales on the horizontal axis.

The volume change behavior observed in the FFTF and PFR-irradiated stress-free tubes is very different, with the FFTF-irradiated HT9 showing a slight positive volume change transient and the PFR-irradiated HT9 showing a large negative volume transient. Although this differing behavior is obviously due to differences in irradiation history, the exact cause is unknown. However, in a previous study, it was shown that four heats of HT9 with only minor differences in composition and fabrication history, displayed vastly different swelling behavior [8], as shown in Fig. 5. Thus, it may not be so surprising that reactor history can also lead to differences in swelling behavior in the same heat of a material.

The observed steady state densification of the MA957 stress-free pressurized tube is also unusual. Several

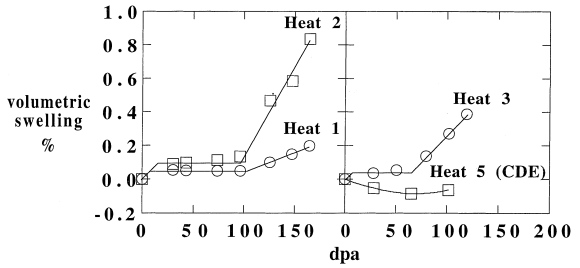

Fig. 5. Estimated swelling from diameter measurements of stress-free tubes of four heats of HT9 irradiated in FFTF [8].

Table 2
Calculated creep coefficients

Alloy	B_0, $\times 10^{-6}$ MPa^{-1} dpa^{-1}	D, $\times 10^{-2}$ MPa^{-1}
FFTF HT9	0.95	0.59
PFR HT9	1.7–1.9	[a]
D57	0.4–0.5	[a]
MA957	0.25–0.60	[a]

[a] No observed swelling.

reasons for this phenomenon may be offered: (1) Residual porosity remaining from the mechanical alloying process may be reclaimed as irradiation proceeds, (2) A precipitation reaction may have occurred, and (3) the unique, highly anisotropic grain structure in this material may be causing this contraction phenomenon. Without microstructural examination, it is impossible to deduce which of these processes caused the densification.

4.2. Irradiation creep

The MA957 also exhibited unusual creep behavior. After creeping at a constant rate for the first 80 dpa, the creep rate appears to decrease during the last irradiation increment. However, the reduction in creep rate is not large. The reason for the reduction in creep rate with increasing dose is not understood at this time.

Irradiation creep was examined from the $\bar{B} = \dot{\bar{\varepsilon}}/\bar{\sigma} = B_0 + D\dot{S}$ creep model, where $\bar{B}$ is the stress-normalized effective creep rate, B_0 the creep compliance, D the creep-swelling coupling coefficient, and $\dot{S}$ the volumetric swelling rate. In absence of any swelling, the creep rate is determined entirely by the creep compliance contribution. The calculated creep coefficients for each of the alloys is reported in Table 2. A creep-swelling coupling coefficient was only calculated for the FFTF-irradiated HT9, as it was the only material that appeared to swell. B_0 for the PFR-irradiated HT9 is higher than previously observed in ferritic alloys and is thought to be related to the large densification observed in the stress-free tube. The creep compliance for D57 and MA957 is within the range of values previously observed in ferritic–martensitic alloys. The range of B_0 values shown for MA957 reflects the decreasing creep rate with increasing dose, whereas the range of values for PFR HT9 and D57 encompasses the values for the tube-sets irradiated in the low and high flux positions in the PFR DMSA.

5. Conclusions

HT9, D57, and MA957 irradiation creep specimens were irradiated in one or both of two fast reactors at ~400°C to doses ranging from ~50 to ~165 dpa. A variety of densification phenomenon was observed. Swelling was apparent only in the FFTF-irradiated HT9. In all cases, irradiation creep was linear with the applied stress. With the exception of the PFR-irradiated HT9, the creep compliance, B_0, fell within the range 0.25–1.0 $\times$ 10^{-6} MPa^{-1} dpa^{-1}, and where it could be measured, the creep-swelling coupling coefficient was found to be 0.6 $\times$ 10^{-2} MPa^{-1}. These values are typical of those from previous irradiation creep studies of ferritic-martensitic alloys. The results of this study and a related study [8] show that phase-related strains in steels like HT9 can be variable, depending on minor details of composition, preparation, and reactor history.

References

[1] A. Kohyama, A. Hishinuma, D.S. Gelles, R.L. Klueh, W. Dietz, K. Ehrlich, J. Nucl. Mater. 233–237 (1996) 138–147.
[2] Proceedings on the IEA Workshop on Ferritic/Martensitic Steels, Tokyo, 1992.
[3] F.A. Garner, Materials Science and Technology, a Comprehensive Treatment, vol. 10a, VCH, Weinheim 1994, p. 507.
[4] M.L. Hamilton, D.S. Gelles, R.J. Lobsinger, M.M. Paxton, W.F. Brown, HEDL-TC-2952, Westinghouse Hanford Company, 1987.
[5] C.L. Dodd et al., paper 20, 28th Irradiation Devices Plenary Meeting, Brasimone, 1984.
[6] M.B. Toloczko, F.A. Garner, J. Standring, B. Munro, S. Adaway, these Proceedings.
[7] E.R. Gilbert, B.A. Chin, Effects of Radiation on Materials: Tenth Conference, ASTM STP 725, American Society for Testing and Materials, 1981, pp. 665–679.
[8] M.B. Toloczko, F.A. Garner, Effects of Irradiation on Materials: 18th International Symposium, ASTM STP 1325, American Society for Testing and Materials, 1997, to be published.
[9] M.B. Toloczko, F.A. Garner, C.R. Eiholzer, J. Nucl. Mater. 212–215 (1994) 604–607.